

LISA-3D: Lifting Language-Image Segmentation to 3D via Multi-View Consistency

Zhongbin Guo, Jiahe Liu, Wenyu Gao, Yushan Li, Chengzhi Li, Ping Jian*
 School of Computer Science & Technology, Beijing Institute of Technology
 {guozhongbin, pjian}@bit.edu.cn

Abstract

*Text-driven 3D reconstruction demands a mask generator that simultaneously understands open-vocabulary instructions and remains consistent across viewpoints. We present **LISA-3D**, a two-stage framework that lifts language-image segmentation into 3D by retrofitting the instruction-following model LISA with geometry-aware Low-Rank Adaptation (LoRA) layers and reusing a frozen SAM-3D reconstructor. During training we exploit off-the-shelf RGB-D sequences and their camera poses to build a differentiable reprojection loss that enforces cross-view agreement without requiring any additional 3D-text supervision. The resulting masks are concatenated with RGB images to form RGBA prompts for SAM-3D, which outputs Gaussian splats or textured meshes without retraining. Across Scan-Refer and Nr3D, LISA-3D improves language-to-3D accuracy by up to +15.6 points over single-view baselines while adapting only 11.6M parameters. The system is modular, data-efficient, and supports zero-shot deployment on unseen categories, providing a practical recipe for language-guided 3D content creation. Our code will be available at <https://github.com/binisalegend/LISA-3D>.*

1. Introduction

The ability to interpret free-form natural language and ground it within three-dimensional environments represents a fundamental challenge at the intersection of computer vision, natural language processing, and 3D reconstruction [3, 10, 19, 23, 28]. This capability is essential for applications ranging from interactive scene editing [29] and robotic manipulation to augmented reality content creation [24] and embodied AI systems [28].

Recent advances in the Segment Anything family [4, 12, 18], particularly SAM3D [25], have demonstrated remarkable capabilities in producing high-fidelity 3D reconstruc-

tions when provided with accurate segmentation masks. However, a critical bottleneck remains: the quality of the input mask fundamentally determines reconstruction quality, and language is seldom translated into pixel-accurate masks without expensive 3D-language supervision. Existing approaches place off-the-shelf mask proposers in front of SAM3D, but treat every image independently, failing to exploit multi-view coherence available in RGB-D sequences. When multiple views are processed in isolation, the resulting masks exhibit inconsistencies that propagate directly into corrupted 3D outputs.

Instruction-following vision-language models such as LISA [13] and Sa2VA [26] offer powerful open-vocabulary visual reasoning, interpreting complex natural language instructions to produce segmentation masks without being limited to a fixed vocabulary. However, these models were designed exclusively on 2D image-text pairs with no mechanism to ensure geometric consistency across viewpoints. When naïvely combining LISA with SAM3D, this lack of multi-view awareness becomes immediately apparent: as illustrated in Figure 1, mask inconsistencies across viewpoints translate directly into reconstruction artifacts such as floating fragments and incomplete surfaces.

This observation motivates our central research question: *Can we retrofit a 2D vision-language model with sufficient geometric awareness to reliably feed SAM3D, while keeping both the VLM backbone and the 3D lifting module frozen?* Freezing these components preserves rich open-vocabulary knowledge, avoids expensive full fine-tuning, and ensures SAM3D’s reconstruction quality remains intact. We answer this question affirmatively by introducing **LISA-3D**, a novel two-stage architecture that bridges the gap between 2D language grounding and 3D reconstruction through geometry-aware adaptation. As illustrated in Figure 1, our framework consists of two sequential stages: (1) *Geometry-Aware Semantic Reasoning*, where a fine-tuned LISA model interprets text instructions to locate target objects across multiple 2D views with enforced consistency; and (2) *Mask-Guided 3D Lifting*, where SAM-3D aggregates these consistent 2D cues to reconstruct explicit 3D entities without additional

*Corresponding Author.

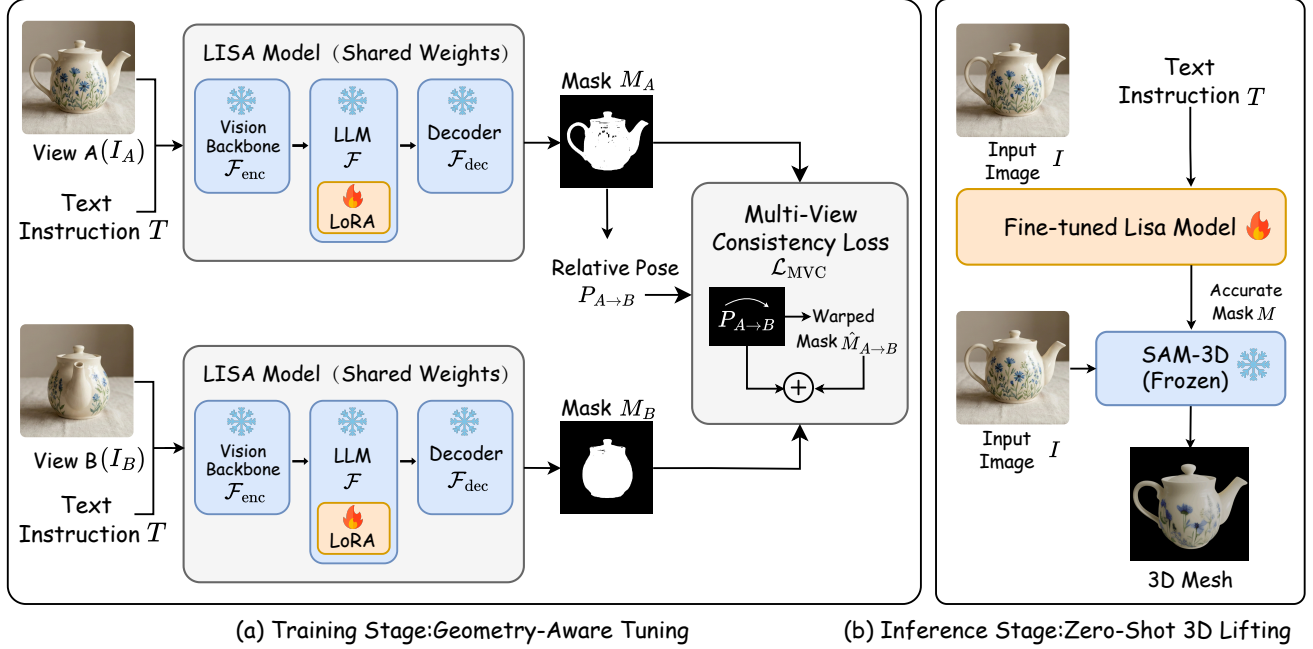


Figure 1. Overview of LISA-3D. Our framework operates in two stages. First, geometry-aware LISA receives multi-view RGB-D pairs and text instructions, producing consistent segmentation masks via LoRA tuning and differentiable warping supervision. The geometric consistency loss enforces that predictions on different views agree when projected through known camera transformations. Second, the predicted masks are concatenated with RGB images to form RGBA prompts for SAM-3D, which reconstructs Gaussian splats or meshes without additional training. This decoupled design preserves the open-vocabulary reasoning of LISA while enabling faithful 3D reconstruction from natural language alone.

training.

The key innovation enabling this architecture lies in our training paradigm. Rather than relying on expensive 3D-text paired datasets, we propose a self-supervised geometric alignment mechanism that leverages the physical laws of rigid body motion as supervision. Specifically, we exploit the multi-view consistency constraint: if a model correctly understands the 3D structure of a scene, its predictions on different views of the same object should be geometrically consistent when projected through known camera transformations. RGB-D sequences naturally provide the necessary ingredients—camera intrinsics, extrinsics, and depth maps—enabling differentiable warping operations that enforce cross-view agreement without requiring any language-3D annotations. To implement this efficiently, we adopt Parameter-Efficient Fine-Tuning (PEFT) through Low-Rank Adaptation (LoRA) [9] modules injected into the attention layers of LISA. By freezing the pretrained weights of both the vision backbone and the language model, we constrain the adaptation to approximately 1.1% of the full model’s parameters while still achieving substantial improvements in multi-view consistency. The LoRA modules learn to modulate attention patterns in a way that implicitly encodes geometric awareness, produc-

ing masks that remain stable across viewpoint changes.

Our training objective combines two complementary terms: a standard 2D segmentation loss that maintains the model’s instruction-following capability using ground truth masks, and our novel geometric consistency loss that penalizes discrepancies between a model’s prediction on one view and the warped prediction from another view. By differentially warping probability maps using depth and camera parameters, we create a self-supervised signal that encourages geometrically coherent outputs without requiring additional annotations beyond what is already available in standard RGB-D datasets.

In the second stage, we leverage the consistent masks produced by geometry-aware LISA to guide SAM-3D reconstruction. Following the input protocol of SAM-3D, we format the visual prompt by concatenating the original RGB image with the predicted binary mask along the channel dimension, creating an RGBA representation that explicitly isolates the object of interest. This mask-conditioned lifting approach allows SAM-3D to focus its reconstruction capacity on the target object, producing clean Gaussian splats or meshes that faithfully represent the language-specified entity. Crucially, SAM-3D remains completely frozen—we use it purely as an off-the-shelf lifting module, demon-

strating that high-quality language-guided 3D reconstruction can be achieved without retraining the 3D component.

The decoupled design of LISA-3D offers several practical advantages: (1) it enables reconstruction of multiple 3D entities from a single scene by simply varying the text instruction; (2) it maintains the open-vocabulary generalization of LISA for novel object categories and complex referring expressions; (3) it preserves the reconstruction quality of SAM-3D; and (4) the lightweight LoRA adaptation makes the approach computationally efficient, requiring only a fraction of the resources needed for full fine-tuning.

Our main contributions are summarized as follows:

- **Geometry-aware LoRA tuning.** We introduce a reprojection-consistency objective that aligns LISA masks across views by differentially warping logits using depth and camera intrinsics.
- **Mask-guided SAM-3D lifting.** We reformat the predicted masks into RGBA prompts and feed them to SAM-3D without re-training, enabling faithful Gaussian or mesh reconstructions from natural language alone.
- **Comprehensive evaluation.** On ScanRefer and Nr3D we outperform LISA fine-tuning baselines while using only 11.6M trainable parameters. Qualitative demos (Figure 2) showcase multi-object and fine-grained referring cases.

2. Methodology

Our goal is to convert a natural-language referring expression into an object-centric 3D representation without retraining a 3D reconstructor or collecting 3D-text pairs. LISA-3D achieves this via two tightly-coupled components: a geometry-aware instruction follower that predicts consistent masks across views, and a mask-guided lifting module that reuses SAM-3D to hallucinate explicit geometry (Figure 1). Below we introduce the notation, architectural details, and training objective.

2.1. Problem Formulation

Given an RGB-D sequence $\{(I_k, D_k, K_k, E_k)\}_{k=1}^N$ captured from the same scene and a referring expression T , we seek per-view masks M_k and corresponding object reconstructions \mathcal{O}_k . Each $I_k \in \mathbb{R}^{H \times W \times 3}$ is an RGB image, $D_k \in \mathbb{R}^{H \times W}$ is a depth map, K_k and E_k respectively denote the intrinsic and extrinsic matrices of view k . The language expression T describes a single instance (e.g., “the blue chair near the window”). Our pipeline (i) grounds T in every I_k using a geometry-aware LISA model Φ_θ with trainable LoRA parameters θ , then (ii) feeds the resulting masks to a frozen SAM-3D reconstructor Ψ to obtain explicit 3D geometry. Importantly, only θ is trained; SAM-3D and the base LISA weights remain intact.

2.2. Geometry-Aware Semantic Reasoning

Let $P_k = \Phi_\theta(I_k, T)$ denote the per-pixel logits before sigmoid. We inject Low-Rank Adaptation (LoRA) modules into every self-attention layer of the vision encoder and the language decoder, yielding trainable matrices (\mathbf{A}, \mathbf{B}) of rank r that modify the original weight \mathbf{W} via $\mathbf{W}' = \mathbf{W} + \alpha \mathbf{A} \mathbf{B}^\top$. This keeps the parameter count under 12M while allowing gradients to flow through both the visual and textual branches.

Multi-view sampling. During training we sample view pairs (a, b) with overlapping fields-of-view. The base LISA is good at semantic alignment but not aware of relative pose; thus we explicitly enforce cross-view consistency.

Differentiable reprojection. For any pixel $\mathbf{u} = (u, v)$ in view a , we compute its 3D point using depth:

$$\mathbf{x}_{3D} = D_a(\mathbf{u}) \cdot K_a^{-1}[u, v, 1]^\top. \quad (1)$$

We transform it into the coordinate system of view b via

$$\tilde{\mathbf{x}} = E_b E_a^{-1} \begin{bmatrix} \mathbf{x}_{3D} \\ 1 \end{bmatrix}, \quad (2)$$

and reproject to the image plane:

$$\mathbf{u}' = \pi(\tilde{\mathbf{x}}) = \frac{K_b[\tilde{x}, \tilde{y}, \tilde{z}]^\top}{\tilde{z}}. \quad (3)$$

Using bilinear interpolation implemented through `grid_sample`, we build a warping operator \mathcal{W} that maps logits from view a to b :

$$\tilde{P}_{a \rightarrow b} = \mathcal{W}(P_a, D_a, K_a, E_a, K_b, E_b). \quad (4)$$

Symmetrically we obtain $\tilde{P}_{b \rightarrow a}$.

Loss function. We maintain instruction fidelity by supervising each view with ground-truth masks M_a, M_b (derived from 3D annotations) via the standard BCE+Dice loss:

$$\mathcal{L}_{seg} = \text{BCE}(P_a, M_a) + \text{Dice}(P_a, M_a) + (a \leftrightarrow b). \quad (5)$$

To enforce geometry, we measure the discrepancy between view b logits and the warped prediction from view a :

$$\mathcal{L}_{geo} = \|P_b - \text{stopgrad}(\tilde{P}_{a \rightarrow b})\|_1 + \|P_a - \text{stopgrad}(\tilde{P}_{b \rightarrow a})\|_1, \quad (6)$$

where stopgradient prevents trivial solutions (e.g., collapsing both predictions to zero). The total loss is

$$\mathcal{L}_{total} = \mathcal{L}_{seg} + \lambda \mathcal{L}_{geo}, \quad (7)$$

with $\lambda = 0.4$ in all experiments. Only the LoRA parameters θ are updated.

Why multi-view consistency matters. Without \mathcal{L}_{geo} , the network may satisfy supervision by inventing view-specific masks. Because SAM-3D expects tight RGBA prompts, small inconsistencies cause severe artifacts (ghost objects, missing parts). Our geometric loss propagates pose information into the VLM, effectively turning LISA into a geometry-aware referential segmenter.

2.3. Mask-Guided 3D Lifting

SAM-3D [25] takes RGBA images where the alpha channel specifies the reconstruction target. Given the logits P_k , we derive a binary mask $M_k = 1 (P_k > \tau)$ with $\tau = 0.5$ and concatenate it with the RGB channels:

$$I_k^{prompt} = [I_k, M_k] \in \mathbb{R}^{H \times W \times 4}. \quad (8)$$

The SAM-3D pipeline first samples sparse structures, then refines them into Gaussian splats and meshes. We do not modify any SAM-3D weights; instead, accurate masks implicitly localize the object, allowing the reconstructor to focus on geometry. For scenes containing multiple expressions, we repeat the lifting step independently and optionally fuse the resulting Gaussians.

2.4. Training and Inference Pipeline

Algorithm below summarizes the procedure. During inference, only a single image I and text T are required; multi-view batches are used solely to train θ .

Training Procedure.

1. Sample scene s and two frames $(I_a, D_a, K_a, E_a), (I_b, D_b, K_b, E_b)$ with referring text T .
2. Predict logits $P_a = \Phi_\theta(I_a, T), P_b = \Phi_\theta(I_b, T)$.
3. Compute \mathcal{L}_{seg} using projected ground-truth masks M_a, M_b .
4. Warp logits via \mathcal{W} to obtain $\tilde{P}_{a \rightarrow b}, \tilde{P}_{b \rightarrow a}$ and compute \mathcal{L}_{geo} .
5. Update LoRA parameters θ with gradients of \mathcal{L}_{total} .

Inference. Given a single image I and text T , obtain mask $M = 1 (P > 0.5)$, form $I^{prompt} = [I, M]$, and execute SAM-3D lifting: $\mathcal{O} = \Psi(I^{prompt}, K, E)$.

2.5. Complexity Considerations

Our approach adds negligible overhead: the reprojection loss uses off-the-shelf `grid_sample`, and the LoRA tuning introduces only $\sim 11.6M$ trainable parameters. SAM-3D inference remains unchanged, so the entire system inherits its reconstruction speed (typically < 40 seconds for Gaussian splats [11]). This makes LISA-3D an attractive drop-in upgrade for any workflow already using SAM-3D but lacking reliable text-grounded masks.

3. Experiments

3.1. Data Sources and Pre-processing

We curate ScanRefer training dataset of RGB-D data to validate our method. ScanRefer [5] provides 800 ScanNet [8] scenes paired with textual descriptions. Instead of using the full noisy raw data, we adopt filtered training split, which contains approximately 27k high-quality utterance-view pairs where the target object is strictly visible and holds valid depth information. This filtering ensures that the reprojection supervision remains reliable. We evaluate on the official validation split. Data pre-processing follows standard protocols: RGB frames are resized to 1024×1024 with padding. Depth maps are clipped to $[0.2, 5.0]$ m.

3.2. Implementation Details

We initialize our model from LISA [13]. We inject LoRA adapters ($r = 16, \alpha = 32$) into all attention layers of the vision and language branches. The model is trained using AdamW [16] with a learning rate of 3×10^{-4} and weight decay of 0.05. The batch size is set to 2 views per GPU (total effective batch size 32 across 4 RTX 6000 Ada GPUs). The geometric consistency weight λ is set to 0.4. During inference, we sample two views per instruction, fuse predictions via our warping operator, and threshold the final mask at 0.5 before passing it to the frozen SAM-3D.

3.3. Benchmarks and Metrics

We evaluate on two benchmarks:

ScanRefer. A large-scale dataset of indoor RGB-D sequences paired with free-form referring expressions.

Nr3D. [1] A benchmark focusing on object-level referring expressions grounded in real indoor environments. The instructions emphasize fine-grained distinctions between nearby objects, making it a challenging test of both language grounding and geometric reasoning.

To assess segmentation and reconstruction quality, we report three complementary metrics:

2D mIoU. (\uparrow) The mean Intersection-over-Union between predicted masks and the ground-truth 2D projections. This metric directly reflects the quality of language-conditioned segmentation, and serves as the foundation for 3D lifting.

F-score. (\uparrow) Computed between the reconstructed point cloud and the ground-truth object surface after alignment. This score captures the geometric completeness and precision of the lifted 3D representation.

Chamfer Distance (CD). (\downarrow , scaled by 10^2) The symmetric Chamfer Distance between reconstructed and ground-truth point sets. Lower values signify more accurate spatial alignment and fewer structural artifacts in the predicted geometry.

Table 1. Quantitative evaluation on 3D referring expression comprehension. 2D mIoU measures mask prediction quality. F-Score and CD (Chamfer Distance, normalized, $\times 10^2$, lower is better) evaluate 3D reconstruction quality.

Method	ScanRefer			Nr3D		
	2D mIoU \uparrow	F-Score \uparrow	CD \downarrow	2D mIoU \uparrow	F-Score \uparrow	CD \downarrow
LISA (2D Baseline)	10.2	–	–	11.2	–	–
LISA + SAM3D	10.2	54.7	12.4	11.2	53.4	12.2
LISA-Geo (Ours, 1-view)	17.6	61.8	10.2	18.3	60.5	10.5
LISA-3D (Ours, Multi-view)	25.4	70.3	7.9	26.1	68.7	8.2

Since LISA (2D Baseline) produces only 2D segmentation masks without 3D lifting, it is evaluated solely with 2D mIoU.

3.4. Baselines

We compare LISA-3D against the following variants to demonstrate the effectiveness of our lifting strategy:

- **LISA (2D Baseline):** The original LISA model applied per-frame. The 3D mask is obtained by simple depth back-projection without any cross-view fusion.
- **LISA + SAM-3D (Naive):** We feed the independent per-frame masks from the vanilla LISA directly into SAM-3D. This tests the capability of SAM-3D to handle inconsistent prompts.
- **LISA-Geo (Single View):** Our model trained with the reprojection loss but inferred using only a single view, verifying the benefit of geometric-aware tuning.
- **LISA-3D (Ours):** The full pipeline using multi-view training and multi-view inference with the proposed consistency constraint.

3.5. Quantitative Results

Table 1 summarizes the results on ScanRefer and Nr3D. The 2D LISA baseline yields very low 2D mIoU (10.2 on ScanRefer, 11.2 on Nr3D), confirming the difficulty of resolving language-grounded segmentation with purely 2D reasoning. Adding SAM-3D (“LISA + SAM3D”) improves reconstruction accuracy, but the overall geometry remains noisy due to inconsistent per-frame masks, as reflected by moderate F-scores and high CD.

Introducing geometric supervision (LISA-Geo) significantly improves both segmentation and reconstruction: mIoU increases by over 7 points, and CD drops from 12.4 to 10.2 on ScanRefer. This demonstrates that enforcing reprojection alignment during training directly enhances mask reliability.

Our full LISA-3D model achieves the strongest performance on all metrics across both datasets. On ScanRefer, LISA-3D reaches 25.4 mIoU, 70.3 F-score, and 7.9 CD, representing substantial gains over both LISA + SAM3D and LISA-Geo. Similar improvements are observed on Nr3D (26.1 mIoU, 68.7 F-score, 8.2 CD), highlighting the

Table 2. Ablation on view count and geometric loss. 2D mIoU and F-Score are evaluated on ScanRefer validation set. Runtime is measured per training iteration on RTX 6000 Ada.

Configuration	2D mIoU \uparrow	F-Score \uparrow	Runtime (s) \downarrow
1 view, w/o \mathcal{L}_{geo}	10.2	54.7	0.72
1 view, + \mathcal{L}_{geo}	17.6	61.8	0.81
2 views, + \mathcal{L}_{geo}	25.4	70.3	0.96
3 views, + \mathcal{L}_{geo}	26.2	71.1	1.28

robustness of our geometric-consistency framework and the effectiveness of multi-view inference.

3.6. Qualitative Observations

Figure 2 depicts representative cases. LISA-3D retrieves multiple chairs described by subtle relational clauses (“the object that the players in the foreground are currently competing for?”), producing disjoint RGBA prompts that SAM-3D turns into separate Gaussian splats. In contrast, the single-view baselines frequently merge adjacent objects or misinterpret occluded instances, which results in broken reconstructions.

4. Analysis and Ablations

4.1. Impact of Multi-view Supervision

We analyze the contribution of multi-view supervision and the geometric consistency loss \mathcal{L}_{geo} using the ScanRefer validation set. Results are summarized in Table 2.

Effect of geometric consistency. Comparing the single-view settings (Row 1 and Row 2), introducing \mathcal{L}_{geo} yields substantial improvements in both 2D mIoU (10.2 \rightarrow 17.6) and F-score (54.7 \rightarrow 61.8). This demonstrates that enforcing cross-view reprojection compatibility, even when only a single view is used at inference, acts as an effective regularizer that encourages spatially coherent mask predictions.

Effect of the number of training views. Moving from 1 to 2 views (Row 2 and Row 3) produces the largest gain, improving 2D mIoU by +7.8 and F-score by +8.5. Explicit multi-view warping enables the model to correct viewpoint-specific errors and capture more stable object boundaries.



Figure 2. Qualitative demos. From left to right: input image, LISA-3D mask, SAM-3D reconstruction (Gaussian splat) and textured mesh. Our geometry-aware LoRA ensures precise localization even for fine-grained referring expressions.

Adding a third view (Row 4) provides only marginal improvements (+0.8 mIoU, +0.8 F-score) while increasing per-iteration runtime from 0.96 \rightarrow 1.28 (+33%). This diminishing return suggests that two views offer the best trade-off between performance and efficiency, and we therefore adopt the 2-view configuration for all main experiments.

4.2. Interface to SAM-3D

We further investigate how the form of the mask prompt affects reconstruction quality in SAM-3D. Two prompting strategies are compared: soft probability maps, where

SAM-3D receives continuous per-pixel scores, and discrete masks obtained after converting probabilities into binary spatial support.

Although soft maps preserve uncertainty and offer theoretically richer supervision, they consistently degrade the reconstruction quality. The continuous activations cause spatial leakage in the Gaussian splatting stage, leading to blurred object boundaries and inflated Chamfer Distance. The splatting process interprets low-confidence background pixels as partial foreground support, accumulating noise in 3D space.

In contrast, discrete masks provide a compact and spa-

tially stable object region, enabling SAM-3D to produce cleaner and more consistent point-level reconstructions. This results in higher F-scores and lower geometric error across all evaluated scenes.

We additionally explored an embedding-level interface, in which LISA’s latent segmentation token is streamed directly into SAM-3D. While promising for future end-to-end pipelines, this approach currently underperforms binary mask prompting due to a mismatch between the latent space of LISA and the spatially structured input expected by SAM-3D.

5. Related Work

Text-guided object grounding in 3D. Early efforts such as ScanRefer [5] and ReferIt3D [1] focus on grounding language in reconstructed ScanNet [8] meshes by predicting 3D bounding boxes or point sets. Subsequent methods couple 3D detectors with transformers, e.g., Point-gnn [22] and InstanceRefer [27], but they still require expensive point-cloud encoders and are hard to deploy on raw RGB imagery. The Segment Anything family [4, 12, 18] provides promptable segmentation from points, boxes, or masks; SAM3D [25] extends the paradigm to 3D lifting via sparse structure sampling. Our approach is orthogonal: we repurpose a 2D instruction follower (LISA) and enforce geometric priors through differentiable reprojection, thereby avoiding full-fledged 3D feature extractors.

Vision-language models with segmentation heads. LISA [13] extends LLaVA [15] by attaching a SAM-style decoder, enabling instruction-based segmentation on 2D datasets. Other works, e.g., Grounded-SAM [20], combine CLIP [17] with SAM [12] for bounding box and mask generation. These methods excel in single-view perception but falter in scenes where depth or pose must be respected. Our reprojection loss can be seen as injecting physical constraints into such VLMs [2]: it prevents shortcuts and ensures that the same textual instruction is grounded in the same object across cameras.

Language-guided 3D reconstruction. Diffusion-based systems like SDFusion [6], Anything-3D [21] produce shapes from textual prompts but often hallucinate coarse geometry and require heavy training. Part-aware methods such as Part123 [14] or LAM3D [7] improve structural fidelity, yet they still depend on large 3D annotations. LISA-3D sidesteps these costs: we reuse a powerful reconstructor (SAM3D) and feed it reliable language-grounded masks learned via self-supervised geometry. In summary, prior art either keeps 2D mask proposers frozen or trains bespoke 3D nets from scratch. LISA-3D contributes a third paradigm: retrofitting a mature VLM with multi-view consistency so that a frozen 3D lifter can be used unchanged.

6. Limitations and Future Work

While LISA-3D substantially advances language-driven 3D reconstruction, several limitations remain.

Dependence on RGB-D captures. Our geometry loss relies on depth and camera poses. Commodity datasets (ScanRefer, Nr3D) provide these signals, but in-the-wild videos may not. A natural extension is to use monocular depth/pose estimators or to jointly learn them; however, estimation errors could destabilize the reprojection loss. Future work can investigate uncertainty-aware warping or bundle-adjustment style objectives.

Two-stage pipeline. We currently pass hard binary masks to SAM3D. Although modular, this design may discard useful cues encoded in the SEG-token embeddings (e.g., fine-grained semantics, confidence). An exciting direction is to replace the explicit mask concatenation with a learned interface: directly feed the hidden states corresponding to SEG tokens into SAM3D’s prompt encoder, allowing the reconstructor to condition on richer language-aware features. This would effectively collapse the two-stage pipeline and reduce latency while preserving interpretability.

Static scenes and single objects. SAM3D excels at rigid objects; articulated humans or scenes with strong inter-object occlusions remain challenging. Moreover, we lift each referred object independently, ignoring mutual constraints (e.g., “the chair touching the table”). Future extensions could enforce relational priors, or build multi-object Gaussian fields by jointly optimizing multiple RGBA prompts.

Limited open-vocabulary evaluation. Our experiments focus on indoor datasets where vocabulary overlaps with LISA’s pre-training. Deploying the system outdoors or on long-tail categories may expose weaknesses. Collecting language-annotated RGB-D videos with diverse appearances, or augmenting prompts with large-language-model paraphrases, could mitigate this issue.

Toward end-to-end training. A more ambitious research path is to fine-tune SAM3D (or a lighter 3D decoder) directly using gradients from the SEG-token embeddings, bypassing the explicit SAM step. This would require differentiable rendering losses and careful regularization to avoid catastrophic forgetting, yet it might unlock higher fidelity and enable the reconstructor to exploit textual subtleties beyond binary masks.

We hope these discussions motivate future work that blends vision-language reasoning with 3D reconstruction even more tightly, ultimately enabling conversational 3D content creation in unconstrained environments.

7. Conclusion

We have shown that reliable multi-view masks are the key ingredient linking instruction-following segmentation and high-fidelity 3D reconstruction. By injecting geometry-aware LoRA modules into LISA, LISA-3D produces pose-consistent masks that can drive a frozen SAM-3D reconstructor without bespoke 3D training. Extensive experiments confirm that this decoupled design outperforms 2D-only and single-view baselines on standard benchmarks while preserving the open-vocabulary strengths of the underlying VLM. The resulting pipeline remains lightweight (11.6M tunable parameters), inherits SAM-3D’s reconstruction quality, and enables downstream applications such as multi-object lifting and zero-shot transfer to new domains. Looking ahead, tighter coupling—e.g., passing SEG-token embeddings directly into SAM-3D’s prompt encoder—could further reduce latency and open the door to fully differentiable, single-stage language-to-3D models. Overall, LISA-3D demonstrates that geometry-aware adaptation is a powerful route toward practical, modular, and scalable 3D understanding from natural language.

References

- [1] Panos Achlioptas, Ahmed Abdelreheem, Fei Xia, Mohamed Elhoseiny, and Leonidas Guibas. ReferIt3D: Neural Listeners for Fine-Grained 3D Object Identification in Real-World Scenes. In *Computer Vision – ECCV 2020*, pages 422–440. Springer International Publishing, Cham, 2020. 4, 7
- [2] Shuai Bai, Keqin Chen, Xuejing Liu, Jialin Wang, Wenbin Ge, Sibao Song, Kai Dang, Peng Wang, Shijie Wang, Jun Tang, Humen Zhong, Yuanzhi Zhu, Mingkun Yang, Zhao-hai Li, Jianqiang Wan, Pengfei Wang, Wei Ding, Zheren Fu, Yiheng Xu, Jiabo Ye, Xi Zhang, Tianbao Xie, Zesen Cheng, Hang Zhang, Zhibo Yang, Haiyang Xu, and Junyang Lin. Qwen2.5-VL Technical Report, 2025. 7
- [3] Ang Cao, Sergio Arnaud, Oleksandr Maksymets, Jianing Yang, Ayush Jain, Ada Martin, Vincent-Pierre Berges, Paul McVay, Ruslan Partsey, Aravind Rajeswaran, Franziska Meier, Justin Johnson, Jeong Joon Park, and Alexander Sax. From thousands to billions: 3d visual language grounding via render-supervised distillation from 2d VLMs. In *Forty-second International Conference on Machine Learning*, 2025. 1
- [4] Nicolas Carion, Laura Gustafson, Yuan-Ting Hu, Shoubhik Debnath, Ronghang Hu, Didac Suris, Chaitanya Ryali, Kalyan Vasudev Alwala, Haitham Khedr, Andrew Huang, Jie Lei, Tengyu Ma, Baishan Guo, Arpit Kalla, Markus Marks, Joseph Greer, Meng Wang, Peize Sun, Roman Rädle, Triantafyllos Afouras, Effrosyni Mavroudi, Katherine Xu, Tsung-Han Wu, Yu Zhou, Liliane Momeni, Rishi Hazra, Shuangrui Ding, Sagar Vaze, Francois Porcher, Feng Li, Siyuan Li, Aishwarya Kamath, Ho Kei Cheng, Piotr Dollár, Nikhila Ravi, Kate Saenko, Pengchuan Zhang, and Christoph Feichtenhofer. SAM 3: Segment Anything with Concepts, 2025. 1, 7
- [5] Dave Zhenyu Chen, Angel X Chang, and Matthias Nießner. Scanrefer: 3d object localization in rgb-d scans using natural language. In *European conference on computer vision*, pages 202–221. Springer, 2020. 4, 7
- [6] Yen-Chi Cheng, Hsin-Ying Lee, Sergey Tulyakov, Alexander G Schwing, and Liang-Yan Gui. Sdfusion: Multimodal 3d shape completion, reconstruction, and generation. In *Proceedings of the IEEE/CVF conference on computer vision and pattern recognition*, pages 4456–4465, 2023. 7
- [7] Ruikai Cui, Xibin Song, Weixuan Sun, Senbo Wang, Weizhe Liu, Shenzhou Chen, Taizhang Shang, Yang Li, Nick Barnes, Hongdong Li, et al. Lam3d: Large image-point clouds alignment model for 3d reconstruction from single image. *Advances in Neural Information Processing Systems*, 37:4454–4480, 2024. 7
- [8] Angela Dai, Angel X Chang, Manolis Savva, Maciej Halber, Thomas Funkhouser, and Matthias Nießner. Scannet: Richly-annotated 3d reconstructions of indoor scenes. In *Proceedings of the IEEE conference on computer vision and pattern recognition*, pages 5828–5839, 2017. 4, 7
- [9] Edward J Hu, Yelong Shen, Phillip Wallis, Zeyuan Allen-Zhu, Yuanzhi Li, Shean Wang, Lu Wang, Weizhu Chen, et al. Lora: Low-rank adaptation of large language models. *ICLR*, 1(2):3, 2022. 2
- [10] Baoxiong Jia, Yixin Chen, Huangyue Yu, Yan Wang, Xuesong Niu, Tengyu Liu, Qing Li, and Siyuan Huang. SceneVerse: Scaling 3D Vision-Language Learning for Grounded Scene Understanding. In *Computer Vision – ECCV 2024*, pages 289–310. Springer Nature Switzerland, Cham, 2025. 1
- [11] Bernhard Kerbl, Georgios Kopanas, Thomas Leimkühler, and George Drettakis. 3d gaussian splatting for real-time radiance field rendering. *ACM Trans. Graph.*, 42(4):139–1, 2023. 4
- [12] Alexander Kirillov, Eric Mintun, Nikhila Ravi, Hanzi Mao, Chloe Rolland, Laura Gustafson, Tete Xiao, Spencer Whitehead, Alexander C. Berg, Wan-Yen Lo, Piotr Dollár, and Ross Girshick. Segment Anything, 2023. 1, 7
- [13] Xin Lai, Zhuotao Tian, Yukang Chen, Yanwei Li, Yuhui Yuan, Shu Liu, and Jiaya Jia. LISA: Reasoning Segmentation via Large Language Model, 2024. 1, 4, 7
- [14] Anran Liu, Cheng Lin, Yuan Liu, Xiaoxiao Long, Zhiyang Dou, Hao-Xiang Guo, Ping Luo, and Wenping Wang. Part123: part-aware 3d reconstruction from a single-view image. In *ACM SIGGRAPH 2024 Conference Papers*, pages 1–12, 2024. 7
- [15] Haotian Liu, Chunyuan Li, Qingyang Wu, and Yong Jae Lee. Visual instruction tuning. *Advances in neural information processing systems*, 36:34892–34916, 2023. 7
- [16] Ilya Loshchilov and Frank Hutter. Decoupled weight decay regularization. *arXiv preprint arXiv:1711.05101*, 2017. 4
- [17] Alec Radford, Jong Wook Kim, Chris Hallacy, Aditya Ramesh, Gabriel Goh, Sandhini Agarwal, Girish Sastry, Amanda Askell, Pamela Mishkin, Jack Clark, et al. Learning transferable visual models from natural language supervision. In *International conference on machine learning*, pages 8748–8763. Pmlr, 2021. 7

- [18] Nikhila Ravi, Valentin Gabeur, Yuan-Ting Hu, Ronghang Hu, Chaitanya Ryali, Tengyu Ma, Haitham Khedr, Roman Rädle, Chloe Rolland, Laura Gustafson, Eric Mintun, Junting Pan, Kalyan Vasudev Alwala, Nicolas Carion, Chao-Yuan Wu, Ross Girshick, Piotr Dollár, and Christoph Feichtenhofer. SAM 2: Segment Anything in Images and Videos, 2024. [1](#), [7](#)
- [19] Ruilong Ren, Xinyu Zhao, Weichen Xu, Jian Cao, Xinxin Xu, and Xing Zhang. A survey of language-grounded multimodal 3d scene understanding. *Knowledge-Based Systems*, 321:113650, 2025. [1](#)
- [20] Tianhe Ren, Shilong Liu, Ailing Zeng, Jing Lin, Kunchang Li, He Cao, Jiayu Chen, Xinyu Huang, Yukang Chen, Feng Yan, et al. Grounded sam: Assembling open-world models for diverse visual tasks. *arXiv preprint arXiv:2401.14159*, 2024. [7](#)
- [21] Qiuhong Shen, Xingyi Yang, and Xinchao Wang. Anything-3d: Towards single-view anything reconstruction in the wild. *arXiv preprint arXiv:2304.10261*, 2023. [7](#)
- [22] Weijing Shi and Raj Rajkumar. Point-gnn: Graph neural network for 3d object detection in a point cloud. In *Proceedings of the IEEE/CVF conference on computer vision and pattern recognition*, pages 1711–1719, 2020. [7](#)
- [23] Ola Shorinwa, Johnathan Tucker, Aliyah Smith, Aiden Swann, Timothy Chen, Roya Firoozi, Monroe Kennedy Iii, and Mac Schwager. Splat-MOVER: Multi-Stage, Open-Vocabulary Robotic Manipulation via Editable Gaussian Splatting. [1](#)
- [24] Andrew Nichols Crawford Taylor. Natural Language Guided Goals for Robotic Manipulation. [1](#)
- [25] D Team, Xingyu Chen, Fu-Jen Chu, Pierre Gleize, Kevin J Liang, Alexander Sax, Hao Tang, Weiyao Wang, Michelle Guo, Thibaut Hardin, Xiang Li, Aohan Lin, Jiawei Liu, Ziqi Ma, Anushka Sagar, Bowen Song, Xiaodong Wang, Jianing Yang, Bowen Zhang, Piotr Dollár, Georgia Gkioxari, and Jitendra Malik. SAM 3D: 3Dfy Anything in Images. [1](#), [4](#), [7](#)
- [26] Haobo Yuan, Xiangtai Li, Tao Zhang, Yueyi Sun, Zilong Huang, Shilin Xu, Shunping Ji, Yunhai Tong, Lu Qi, Jiashi Feng, and Ming-Hsuan Yang. Sa2VA: Marrying SAM2 with LLaVA for Dense Grounded Understanding of Images and Videos, 2025. [1](#)
- [27] Zhihao Yuan, Xu Yan, Yinghong Liao, Ruimao Zhang, Sheng Wang, Zhen Li, and Shuguang Cui. Instancerefer: Cooperative holistic understanding for visual grounding on point clouds through instance multi-level contextual referring. In *Proceedings of the IEEE/CVF International Conference on Computer Vision*, pages 1791–1800, 2021. [7](#)
- [28] Haoyu Zhen, Xiaowen Qiu, Peihao Chen, Jincheng Yang, Xin Yan, Yilun Du, Yining Hong, and Chuang Gan. 3D-VLA: A 3D Vision-Language-Action Generative World Model. <https://arxiv.org/abs/2403.09631v1>, 2024. [1](#)
- [29] Kaizhi Zheng, Xiaotong Chen, Xuehai He, Jing Gu, Linjie Li, Zhengyuan Yang, Kevin Lin, Jianfeng Wang, Lijuan Wang, and Xin Eric Wang. EditRoom: LLM-parameterized Graph Diffusion for Composable 3D Room Layout Editing, 2025. [1](#)